Int. J. Solids Structures, 1966, Vol. 2, pp. 167 to 180. Pergamon Press Ltd. Printed in Great Britain

# THERMAL BUCKLING OF SHALLOW SHELLS

M. A. MAHAYNI

Department of Mechanics and Aerospace Engineering, The University of Kansas, Lawrence, Kansas

**Abstract**—The large deflection equations for a thin shallow shell are modified to include thermal effects. The temperature is considered to be an arbitrary function of the space coordinates.

The resulting equations are used to study thermal buckling and post-buckling behavior of a simply supported cylindrical shell panel, subjected to a parabolic temperature distribution along its axial direction. It is assumed that the temperature is constant across the thickness of the shell and along its circumferential direction. Buckling charts for various curvatures, $K_y$, and aspect ratios, $\lambda$, are presented for two cases of edge conditions. In one case the edges of the panel are free to displace, and in the second case the edges are restrained.

The critical temperature is found to fall outside the practical temperature range of the material for $K_y \geq 200$ in the free-edge condition and for $K_y \geq 50$ in the restrained-edge condition.

## NOTATION

| | |
|---|---|
| $A_n$ | undermined coefficients in equation (9) |
| $a, b$ | panel dimensions |
| $a_i, b_i$ | functions of the parameters $\lambda$, $K_y$, $\mu$, $\bar{K}$, $P_x$ and $P_y$ defined in the Appendix |
| $c$ | coefficient of thermal expansion |
| $D$ | $\dfrac{Eh^3}{12(1-\mu^2)}$ |
| $E, \mu$ | elastic constants of the shell |
| $e$ | $T\|_{x=0}$ |
| $e_x, e_y, \bar{e}_x, \bar{e}_y$ | average displacements in the $x$ and $y$ directions |
| $f$ | $T\|_{x=a}$ |
| $f_1, f_2$ | functions of the parameters $\lambda$, $K_y$, $\mu$, $\bar{K}$ defined in the Appendix |
| $\bar{f}$ | $\dfrac{cfa^2}{h^2}$ |
| $h$ | thickness of the shell |
| $k$ | $\dfrac{\Delta T}{a^2} = \dfrac{e-f}{a^2}$ |
| $k_x, k_y$ | curvatures in $x$ and $y$ direction |
| $K_y$ | $\dfrac{k_y b^2}{h} = \dfrac{b^2}{Rh}$ |
| $\bar{K}$ | $\dfrac{a^2 b^2}{h^2} ck$ |
| $M_T$ | $cE\int_{-h/2}^{h/2} Tz\,dz$ |
| $N_T$ | $cE\int_{-h/2}^{h/2} T\,dz$ |

| | |
|---|---|
| $P_x$ | $\frac{\alpha b^2}{Eh^2}$ |
| $P_y$ | $\frac{\beta a^2}{Eh^2}$ |
| $Q$ | error function |
| $q$ | intensity of lateral load |
| $R$ | radius of curvature |
| $T$ | temperature function |
| $u, v, w$ | displacement components in the $x, y, z$ directions respectively |
| $Z_n$ | $\frac{A_n}{h}$ |
| $\phi$ | Airy stress function |
| $\alpha, \beta$ | average in-plane forces at the edges of the panel |
| $\lambda$ | $\frac{a}{b}$ |

## INTRODUCTION

BECAUSE thermal stresses are assuming major importance in aerospace structures, their determination has attracted widespread interest. Numerous references on thermal stability of shells are reviewed by Anderson [1]. Most of the existing work is concerned with the effect of thermal stresses on the stability of cylinders and cones [2–6].

The present investigation considers the stability of a simply supported, shallow, cylindrical shell panel subjected to non-uniform temperature distribution. The temperature varies along the axial direction of the shell only.

Since the post-buckling behavior of the shell is of primary interest in this investigation, the governing differential equations are based on the non-linear theory. An exact solution of the resulting non-linear problem is not possible. However, an approximate solution is obtained by applying the Galerkin's method.

Numerical results for maximum temperature differences and displacements are determined for two cases of edge conditions. The influence of the curvature parameter and the aspect ratio on the critical temperature is investigated.

## DIFFERENTIAL EQUATIONS

Let $x$ and $y$ be measured along the axial and the circumferential direction in the middle surface of the undeformed shallow shell, Fig. 1. With $u$, $v$ and $w$ as the displacement components of a point in the middle surface, the internal forces can be represented in the following forms, including displacement terms up to second order,

$$N_x = \int_{-h/2}^{h/2} \sigma_x \, dz = \frac{Eh}{1-\mu^2}\left[\frac{\partial u}{\partial x} - k_x w + \frac{1}{2}\left(\frac{\partial w}{\partial x}\right)^2 + \mu\left\{\frac{\partial v}{\partial y} - k_y w + \frac{1}{2}\left(\frac{\partial w}{\partial y}\right)^2\right\}\right] - \frac{N_T}{1-\mu}$$

$$N_y = \int_{-h/2}^{h/2} \sigma_y \, dz = \frac{Eh}{1-\mu^2}\left[\frac{\partial v}{\partial y} - k_y w + \frac{1}{2}\left(\frac{\partial w}{\partial y}\right)^2 \right. \tag{1a}$$

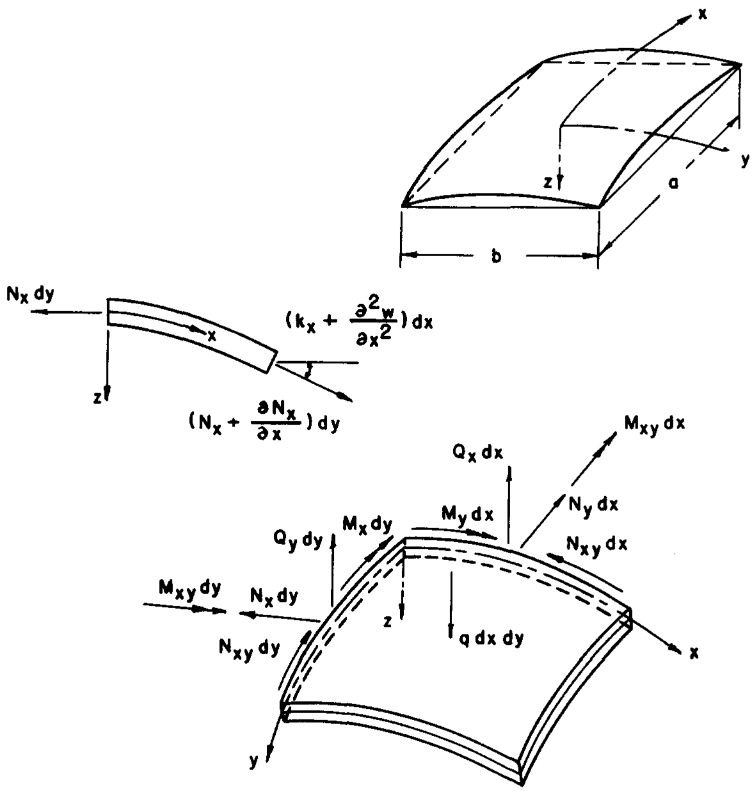


FIG. 1. Geometry of the shell.

$$+\mu\left\{\frac{\partial u}{\partial x}-k_x w+\frac{1}{2}\left(\frac{\partial w}{\partial x}\right)^2\right\}\Bigg]-\frac{N_T}{1-\mu}$$

$$N_{xy}=\int_{-h/2}^{h/2}\tau_{xy}\,\mathrm{d}z=\frac{Eh}{2(1+\mu)}\left[\frac{\partial u}{\partial y}+\frac{\partial v}{\partial x}+\frac{\partial w}{\partial x}\cdot\frac{\partial w}{\partial y}\right]$$

and

$$\begin{aligned} M_x &= -D\left(\frac{\partial^2 w}{\partial x^2}+\mu\frac{\partial^2 w}{\partial y^2}\right)-\frac{M_T}{1-\mu} \\ M_y &= -D\left(\frac{\partial^2 w}{\partial y^2}+\mu\frac{\partial^2 w}{\partial x^2}\right)-\frac{M_T}{1-\mu} \\ M_{xy} &= (1-\mu)D\frac{\partial^2 w}{\partial x\partial y} \end{aligned} \tag{1b}$$

where

$$D=\frac{Eh^3}{12(1-\mu^2)},\ N_T=cE\int_{-h/2}^{h/2}T\,\mathrm{d}z;\quad M_T=cE\int_{-h/2}^{h/2}Tz\,\mathrm{d}z.$$

The equilibrium equations of an element of the shell are

$$
\begin{aligned}
\frac{\partial N_x}{\partial x}+\frac{\partial N_{xy}}{\partial y} &= 0 \\
\frac{\partial N_{xy}}{\partial x}+\frac{\partial N_y}{\partial y} &= 0 \\
\frac{\partial M_x}{\partial x}+\frac{\partial M_{xy}}{\partial y}-Q_x &= 0 \\
\frac{\partial M_{xy}}{\partial x}+\frac{\partial M_y}{\partial y}-Q_y &= 0 \\
\frac{\partial Q_x}{\partial x}+\frac{\partial Q_y}{\partial y}+N_x\left(k_x+\frac{\partial^2 w}{\partial x^2}\right)+N_y\left(k_y+\frac{\partial^2 w}{\partial y^2}\right)+2N_{xy}\frac{\partial^2 w}{\partial x\partial y}+q &= 0
\end{aligned}
\tag{2}
$$

where the following simplified expressions for the change of curvatures and the unit twist of the middle surface are used

$$\chi_x = \frac{\partial^2 w}{\partial x^2}; \qquad \chi_y = \frac{\partial^2 w}{\partial y^2} \quad \text{and} \quad \chi_{xy} = \frac{\partial^2 w}{\partial x\partial y}. \tag{3}$$

The first two equilibrium equations are satisfied identically if

$$N_x = \frac{\partial^2 \phi}{\partial y^2}; \qquad N_y = \frac{\partial^2 \phi}{\partial x^2} \quad \text{and} \quad N_{xy} = -\frac{\partial^2 \phi}{\partial x\partial y} \tag{4}$$

where $\phi$ is the Airy stress function. Eliminating the variables $u$ and $v$ in equations (1a) and (4), the compatibility equation of the shell is obtained

$$\frac{1}{Eh}\nabla^4\phi = \left(\frac{\partial^2 w}{\partial x\partial y}\right)^2-\frac{\partial^2 w}{\partial x^2}\cdot\frac{\partial^2 w}{\partial y^2}-k_x\frac{\partial^2 w}{\partial y^2}-k_y\frac{\partial^2 w}{\partial x^2}-\frac{1}{Eh}\nabla^2 N_T. \tag{5}$$

Expressing the shear forces $Q_x$ and $Q_y$ by the bending moments and taking into account the last three relations (1b) and expressions (4), we obtain from the last equation of group (2) the differential equation

$$D\nabla^4 w = \frac{\partial^2 w}{\partial x^2}\cdot\frac{\partial^2 \phi}{\partial y^2}+\frac{\partial^2 w}{\partial y^2}\cdot\frac{\partial^2 \phi}{\partial x^2}-2\frac{\partial^2 \phi}{\partial x\partial y}\cdot\frac{\partial^2 w}{\partial x\partial y}+k_x\frac{\partial^2 \phi}{\partial y^2}+k_y\frac{\partial^2 \phi}{\partial x^2}+q-\frac{1}{(1-\mu)}\nabla^2 M_T. \tag{6}$$

For the cylindrical shell panel considered, $k_x = 0$ and $k_y = 1/R$, the governing non-linear equations reduce to

$$\frac{1}{Eh}\nabla^4\phi-\left[\left(\frac{\partial^2 w}{\partial x\partial y}\right)^2-\frac{\partial^2 w}{\partial x^2}\cdot\frac{\partial^2 w}{\partial y^2}-\frac{1}{R}\cdot\frac{\partial^2 w}{\partial x^2}-\frac{1}{Eh}\nabla^2 N_T\right] = 0 \tag{7a}$$

$$D\nabla^4 w-\left[\frac{\partial^2 w}{\partial x^2}\cdot\frac{\partial^2 \phi}{\partial y^2}+\frac{\partial^2 w}{\partial y^2}\cdot\frac{\partial^2 \phi}{\partial x^2}-2\frac{\partial^2 \phi}{\partial x\partial y}\cdot\frac{\partial^2 w}{\partial x\partial y}+\frac{1}{R}\cdot\frac{\partial^2 \phi}{\partial x^2}+q-\frac{1}{(1-\mu)}\nabla^2 M_T\right] = 0. \tag{7b}$$

## SOLUTION OF THE PROBLEM

Consider a thin cylindrical shell panel, occupying the space

$$-\frac{a}{2} \leq x \leq \frac{a}{2}; \qquad -\frac{b}{2} \leq y \leq \frac{b}{2} \qquad \text{and} \qquad -\frac{h}{2} \leq z \leq \frac{h}{2}$$

The shell is free of transverse load and is subjected to a temperature distribution governed by the following equation

$$T = [f + k(x-a)^2] \tag{8}$$

where

$$k = \frac{e-f}{a^2} = \frac{\Delta T}{a^2}$$

$$\Delta T = \text{Temperature difference}$$

$$f = T|_{x=a}$$

$$e = T|_{x=0}$$

The edges of the shell are restrained in the transverse direction by simple rigid supports.

A solution of equations (7) which satisfies the boundary conditions is presented in the form of the trignometric series

$$w = \sum_{n=1,2,3\ldots}^{\infty} A_n\left(\cos\frac{\pi x}{a}\cdot\cos\frac{\pi y}{b}\right)^n = \sum_{n=1,2,3\ldots}^{\infty} A_n\psi_n \tag{9}$$

where $A_n$ are undetermined coefficients.

For a first-order solution only the first term of equation (9) is used. The resulting differential equation for $\phi$ becomes

$$\begin{aligned}\frac{1}{Eh}\nabla^4\phi = A_1^2\left(\frac{\pi^2}{ab}\right)^2\left(\sin^2\frac{\pi x}{a}\sin^2\frac{\pi y}{b} - \cos^2\frac{\pi x}{a}\cos^2\frac{\pi y}{b}\right) \\ +\frac{1}{R}\left(\frac{\pi}{a}\right)^2 A_1\cos\frac{\pi x}{a}\cos\frac{\pi y}{b} - ck.\end{aligned} \tag{10}$$

The solution of equation (10) is

$$\begin{aligned}\phi = Eh\left(\frac{\pi^2}{ab}\right)^2\left(-\frac{A_1^2}{2}\right)\left\{\frac{\cos\frac{2\pi x}{a}}{\left(\frac{2\pi}{a}\right)^4} + \frac{\cos\frac{2\pi y}{b}}{\left(\frac{2\pi}{b}\right)^4}\right\} \\ +\frac{Eh}{R}\left(\frac{\pi}{a}\right)^2 A_1\left\{\frac{\cos\frac{\pi x}{a}\cos\frac{\pi y}{b}}{\left[\left(\frac{\pi}{a}\right)^2+\left(\frac{\pi}{b}\right)^2\right]^2}\right\} - \frac{\alpha y^2}{2} - \frac{\beta x^2}{2} - \frac{Ehck}{24}x^4\end{aligned} \tag{11}$$

where $\alpha$ and $\beta$ are the in-plane forces $N_x$ and $N_y$ at the edges of the panel.

The Galerkin method prescribes substituting equations (9) and (11) into equation (7b). In general, the left hand side of equation (7b) will not be zero after this operation. The resulting function on the left hand side is the error function $Q$. To minimize the error the undetermined coefficient of the deflection $w$ must satisfy the integral

$$\int_{-a/2}^{a/2}\int_{-b/2}^{b/2} Q\Psi_n \,dx\,dy = 0. \tag{12}$$

After carrying out the integration of equation (12), simplifying, and introducing the following dimensionless quantities,

$$K_y = \frac{b^2}{Rh}, \qquad \lambda = \frac{a}{b}, \qquad Z_1 = \frac{A_1}{h}$$
$$\bar{K} = \frac{a^2b^2}{h^2}ck, \qquad P_x = \frac{\alpha b^2}{Eh^2} \text{ and } P_y = \frac{\beta a^2}{Eh^2} \tag{13}$$

a cubic equation in $Z_1$ is obtained

$$\frac{\pi^6}{256}\left(\frac{1}{\lambda^2}+\lambda^2\right)Z_1^3 - \left[\frac{2\pi^2}{3}K_y\frac{1}{(\lambda+1/\lambda)^2}+\frac{\pi^2}{24}K_y\lambda^2\right]Z_1^2 + \left[\frac{\pi^2}{16}K_y^2\frac{1}{(\lambda+1/\lambda)^2}\right.$$
$$\left. + \frac{\pi^6}{192(1-\mu^2)}\left(\frac{1}{\lambda}+\lambda\right)^2 - \frac{\pi^4}{16}(P_x+P_y) - \frac{\pi^2}{16}\left(\frac{\pi^2}{6}-\frac{1}{4}\right)\lambda^2\bar{K}\right]Z_1 \tag{14}$$
$$+\left[K_yP_x+\frac{\pi^2-4}{4\pi^2}K_y\bar{K}\lambda^2\right] = 0.$$

To check the convergence of the series equation (9), the second-order solution is obtained and compared to the first-order solution, Fig. 2. In this case the first two terms of equation (9) are considered. The resulting equation for $\phi$ becomes

$$\frac{1}{Eh}\nabla^4\phi = \left(\frac{\pi^2}{ab}\right)^2\left[A_1^2\left\{\sin^2\frac{\pi x}{a}\sin^2\frac{\pi y}{b} - \cos^2\frac{\pi x}{a}\cos^2\frac{\pi y}{b}\right\}\right.$$
$$+2A_1A_2\left\{\sin\frac{\pi x}{a}\sin\frac{2\pi x}{a}\cdot\cos\frac{\pi y}{b}\cos\frac{2\pi y}{b}\right.$$
$$\left.-\cos\frac{\pi x}{a}\cos^2\frac{\pi x}{a}\cos\frac{\pi y}{b}\cdot\cos\frac{2\pi y}{b} - \cos\frac{\pi x}{a}\cos\frac{2\pi x}{a}\cos\frac{\pi y}{b}\cos^2\frac{\pi y}{b}\right\} \tag{15}$$
$$\left.+A_2^3\left\{\sin^2\frac{2\pi x}{a}\sin^2\frac{2\pi y}{b} - 4\cos\frac{2\pi x}{a}\cos^2\frac{\pi x}{a}\cos\frac{2\pi y}{b}\cos^2\frac{\pi y}{b}\right\}\right]$$
$$+\frac{1}{R}\left(\frac{\pi}{a}\right)^2\left[A_1\cos\frac{\pi x}{a}\cos\frac{\pi y}{b}+2A_2\cos\frac{2\pi x}{a}\cos^2\frac{\pi y}{b}\right] - ck.$$

The solution of equation (15) is

$$\phi = Eh\left(\frac{\pi^2}{ab}\right)^2\left[-\frac{A_1^2}{2}\left\{\frac{\cos\frac{2\pi x}{a}}{\left(\frac{2\pi}{a}\right)^4}+\frac{\cos\frac{2\pi y}{b}}{\left(\frac{2\pi}{b}\right)^4}\right\}+2A_1A_2\left\{-\frac{1}{4}\frac{\cos\frac{\pi x}{a}\cos\frac{3\pi y}{b}}{\left[\left(\frac{\pi}{a}\right)^2+\left(\frac{3\pi}{b}\right)^2\right]^2}\right.\right.$$

$$
\begin{aligned}
&-\frac{3}{4}\frac{\cos\frac{\pi y}{b}\cos\frac{3\pi x}{a}}{\left[\left(\frac{\pi}{b}\right)^2+\left(\frac{3\pi}{a}\right)^2\right]^2}-\frac{1}{2}\frac{\cos\frac{3\pi y}{b}\cos\frac{3\pi x}{a}}{\left[\left(\frac{3\pi}{b}\right)^2+\left(\frac{3\pi}{a}\right)^2\right]^2}-\frac{1}{2}\frac{\cos\frac{\pi x}{a}\cos\frac{\pi y}{b}}{\left[\left(\frac{\pi}{a}\right)^2+\left(\frac{\pi}{b}\right)^2\right]^2}\Bigg\}\\
&+A_2^2\left\{-\left(\frac{\cos\frac{2\pi x}{a}}{\left(\frac{2\pi}{a}\right)^4}+\frac{\cos\frac{2\pi y}{b}}{\left(\frac{2\pi}{b}\right)^4}\right)-\frac{1}{2}\frac{\cos\frac{2\pi x}{a}\cos\frac{4\pi y}{b}}{\left[\left(\frac{2\pi}{a}\right)^2+\left(\frac{4\pi}{b}\right)^2\right]^2}-\frac{1}{2}\frac{\cos\frac{2\pi y}{b}\cos\frac{4\pi x}{a}}{\left[\left(\frac{2\pi}{b}\right)^2+\left(\frac{4\pi}{a}\right)^2\right]^2}\right.\\
&\left.-\frac{\cos\frac{2\pi x}{a}\cos\frac{2\pi y}{b}}{\left[\left(\frac{2\pi}{a}\right)^2+\left(\frac{2\pi}{b}\right)^2\right]^2}\right\}\Bigg]+\frac{Eh}{R}\left(\frac{\pi}{a}\right)^2\left[A_1\frac{\cos\frac{\pi x}{a}\cos\frac{\pi y}{b}}{\left[\left(\frac{\pi}{a}\right)^2+\left(\frac{\pi}{b}\right)^2\right]^2}\right.\\
&\left.+A_2\left(\frac{\cos\frac{2\pi x}{a}}{\left(\frac{2\pi}{a}\right)^4}+\frac{\cos\frac{2\pi x}{a}\cos\frac{2\pi y}{b}}{\left[\left(\frac{2\pi}{a}\right)^2+\left(\frac{2\pi}{b}\right)^2\right]^2}\right)\right]-\frac{\alpha y^2}{2}-\frac{\beta x^2}{2}-\frac{Ehck}{24}x^4.
\end{aligned}
\tag{16}
$$

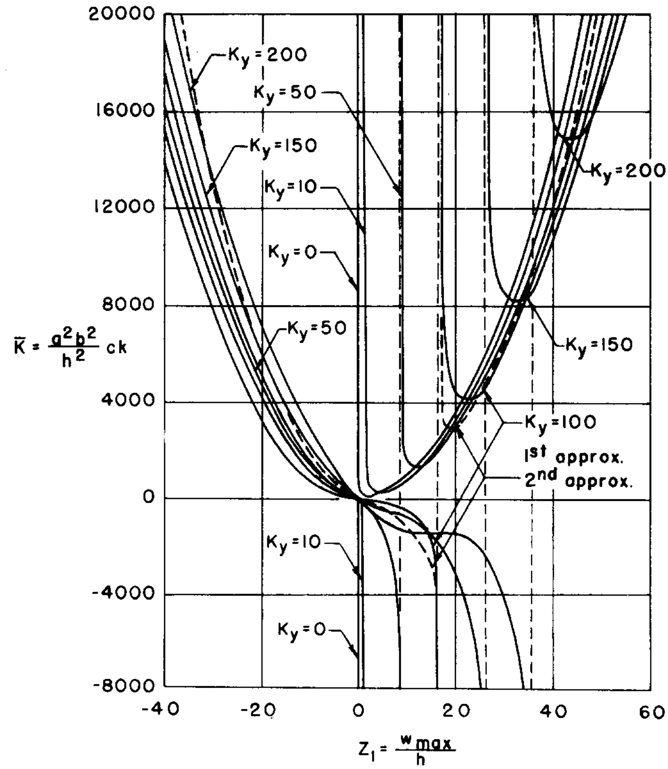


FIG. 2. Load–deflection curve for $\mu = 0{\cdot}3$, $\lambda = 1$ and $P_x = P_y = 0$.

The integration of equation (7b), using the first two terms in equation (9) for $w$ and equation (16) for $\phi$, leads with simplification to the following simultaneous cubic equations in non-dimensional form

$$\begin{aligned} a_1z_1^3+a_2z_1^2z_2+a_3z_1z_2+a_4z_1z_2^2+a_5z_1^2+a_6z_2^2+a_7z_2^3+a_8z_1+a_9z_2 &= f_1(\Delta T) \\ b_1z_1^3+b_2z_1^2z_2+b_3z_1z_2+b_4z_1z_2^2+b_5z_1^2+b_6z_2^2+b_7z_2^3+b_8z_1+b_9z_2 &= f_2(\Delta T) \end{aligned} \quad (17)$$

in which the coefficients $a_i$, $b_i$, $f_1$ and $f_2$ are functions of the parameters $\lambda$, $K_y$, $\mu$, $\bar{K}$, $P_x$ and $P_y$, defined in the Appendix. $Z_1 = A_1/h$ and $Z_2 = A_2/h$.

## NUMERICAL RESULTS

*(a) The edges of the panel are free to displace in its plane*

For this case the end forces $P_x$ and $P_y$ are equal to zero. Hence equation (14) reduces to

$$\frac{\pi^6}{256}\left(\frac{1}{\lambda^2}+\lambda^2\right)Z_1^3-\left[\frac{2\pi^2}{3}K_y\frac{1}{(\lambda+1/\lambda)^2}+\frac{\pi^2}{24}K_y\lambda^2\right]Z_1^2+\left[\frac{\pi^2}{16}K_y^2\frac{1}{(\lambda+1/\lambda)^2}+\frac{\pi^6}{192(1-\mu^2)}\left(\frac{1}{\lambda}+\lambda\right)^2\right.$$
$$\left.-\frac{\pi^2}{16}\left(\frac{\pi^2}{6}-\frac{1}{4}\right)\lambda^2\bar{K}\right]Z_1+\left[\frac{\pi^2-4}{4\pi^2}K_y\bar{K}\lambda^2\right] = 0. \quad (18)$$

The behavior of the shell is best described by plotting graphs of deflection in terms of the maximum temperature difference for various values of the curvature $K_y$ and aspect ratio $\lambda$. The results are shown in Figs. 2 and 3.

The convergence of the series is checked by solving equations (17) for the case where $\lambda = 1$ and $K_y = 100$. The results are plotted in Fig. 2 for comparison.

*(b) The edges of the panel are restrained from displacement in its plane*

The average displacement of the middle surface in the $x$-direction is

$$e_x = -\frac{1}{a}\int_{-a/2}^{+a/2}\frac{\partial u}{\partial x}\,\mathrm{d}x. \quad (19)$$

This average varies in the $y$-direction. Its average over the $y$-coordinate is

$$\bar{e}_x = \frac{1}{b}\int_{-b/2}^{b/2} e_x\,\mathrm{d}y. \quad (20)$$

However

$$\frac{\partial u}{\partial x} = \frac{1}{Eh}\left(\frac{\partial^2\phi}{\partial y^2}-\mu\frac{\partial^2\phi}{\partial x^2}\right)-\frac{1}{2}\left(\frac{\partial w}{\partial x}\right)^2+cT. \quad (21)$$

The substitution of the values of the displacement $w$ and stress function $\phi$ in equation (21) and integrating in accordance with equations (19) and (20) yield in non-dimensional form

$$\bar{e}_x\left(\frac{a}{h}\right)^2 = P_x\lambda^2-\mu P_y+\frac{\pi^2}{8}Z_1^2+\frac{4}{\pi^2}K_yZ_1(\lambda^2-\mu)\cdot\frac{1}{(1/\lambda+\lambda)^2}-\frac{\mu}{24}\lambda^2\bar{K}-\left[\bar{f}+\bar{K}\frac{\lambda^2}{3}\right] \quad (22)$$

where

$$\bar{f} = \frac{cfa^2}{h^2}.$$

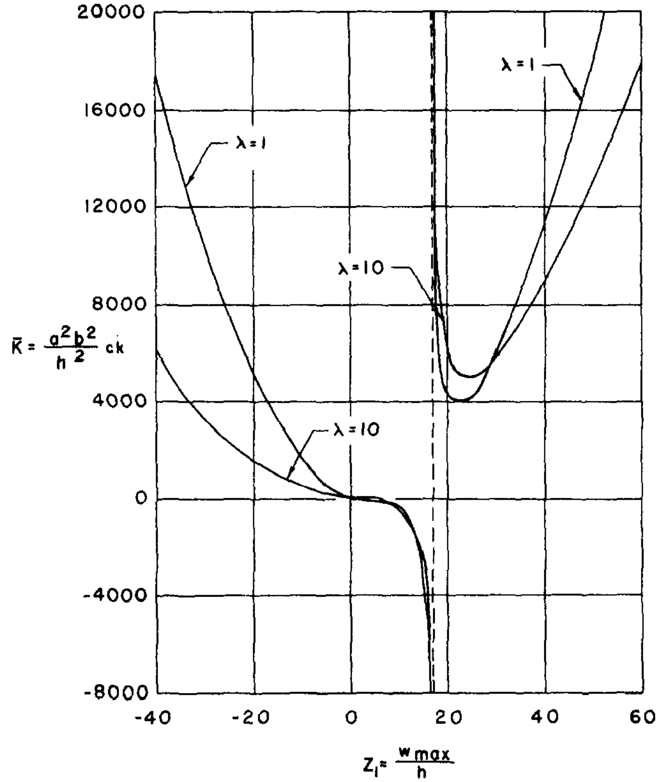


FIG. 3. Load–deflection curve for $\mu = 0{\cdot}3$, $K_y = 100$ and $P_x = P_y = 0$.

Similarly, the average displacement in the $y$-direction is

$$\bar{e}_y\left(\frac{b}{h}\right)^2 = P_y\frac{1}{\lambda^2} - \mu P_x + \frac{\pi^2}{8}Z_1^2 - \frac{4}{\pi^2}K_yZ_1 + \frac{4}{\pi^2}K_yZ_1\cdot\left(\frac{1}{\lambda^2} - \mu\right)\frac{1}{(1/\lambda+\lambda)^2} + \frac{\bar{K}}{24} - \left[\bar{f} + \bar{K}\frac{\lambda^2}{3}\right]. \quad (23)$$

For the panel with restrained edges, the average displacement along the $x$ and $y$-coordinates must vanish.

$$\bar{e}_x = \bar{e}_y = 0.$$

The solution of equations (22) and (23) for this condition yields

$$P_x = -\frac{\pi^2}{8}\left(\frac{1}{\lambda^2} + \mu\right)\frac{1}{1-\mu^2}Z_1^2 + \frac{4}{\pi^2}K_y\left[\frac{\mu}{1-\mu^2} - \frac{1}{(1/\lambda+\lambda)^2}\right]Z_1 + \left(\frac{1}{1-\mu^2}\right)\left(\frac{1}{\lambda^2} + \mu\right)\left(\bar{f} + \frac{\bar{K}\lambda^2}{3}\right)$$

$$\begin{aligned} P_y = &-\frac{\pi^2}{8}(\lambda^2 + \mu)\frac{1}{1-\mu^2}Z_1^2 + \frac{4}{\pi^2}K_y\left[\frac{\lambda^2}{1-\mu^2} - \frac{1}{(1/\lambda+\lambda)^2}\right]Z_1 - \frac{\lambda^2}{24}\bar{K} \\ &+ \left(\frac{1}{1-\mu^2}\right)(\lambda^2 + \mu)\left(\bar{f} + \frac{\bar{K}\lambda^2}{3}\right). \end{aligned} \quad (24)$$

The governing equation for the panel with restrained edges is finally obtained by substituting $P_x$ and $P_y$ in equation (14). The resulting equation is

$$\begin{aligned}&\left\{\frac{\pi^6}{256}\left(\frac{1}{\lambda^2}+\lambda^2\right)+\frac{\pi^6}{128}\frac{1}{1-\mu^2}\left[2\mu+\left(\frac{1}{\lambda^2}+\lambda^2\right)\right]\right\}Z_1^3-\left\{\frac{\pi^2}{6}K_y\frac{1}{(\lambda+1/\lambda)^2}+\frac{\pi^2}{24}K_y\lambda^2\right.\\&\left.+\tfrac{3}{8}\pi^2(\lambda^2+\mu)\frac{K_y}{1-\mu^2}\right\}Z_1^2+\left\{\left(\frac{\pi^2}{16}-\frac{4}{\pi^2}\right)K_y^2\frac{1}{(1/\lambda+\lambda)^2}+\frac{\pi^6}{192(1-\mu^2)}\left(\frac{1}{\lambda}+\lambda\right)^2\right.\\&\left.+\frac{4}{\pi^2}K_y^2\lambda^2\frac{1}{1-\mu^2}+\frac{\pi^2\lambda^2}{64}\bar{K}\left(1-\frac{\pi^2}{2}\right)-\frac{\pi^4}{16}\left(\frac{1}{1-\mu^2}\right)\cdot\left(\bar{f}+\frac{\bar{K}\lambda^2}{3}\right)\left[2\mu+\frac{1}{\lambda^2}+\lambda^2\right]\right\}Z_1\\&+\bar{K}K_y\lambda^2\left(\frac{5}{24}-\frac{1}{\pi^2}\right)+K_y\left(\frac{1}{1-\mu^2}\right)\left(\frac{1}{\lambda^2}+\mu\right)\left(\bar{f}+\frac{\bar{K}\lambda^2}{3}\right)=0.\end{aligned}\tag{25}$$

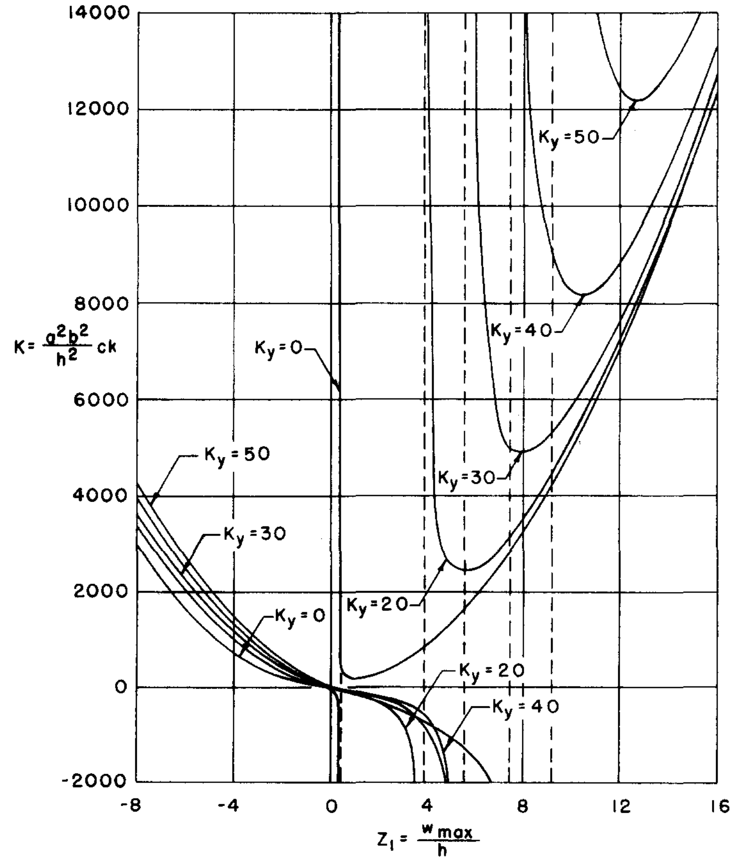


FIG. 4. Load–deflection curve for $\mu = 0{\cdot}3$, $\lambda = 1$, $\bar{f} = 0$ and $\bar{e}_x = \bar{e}_y = 0$.

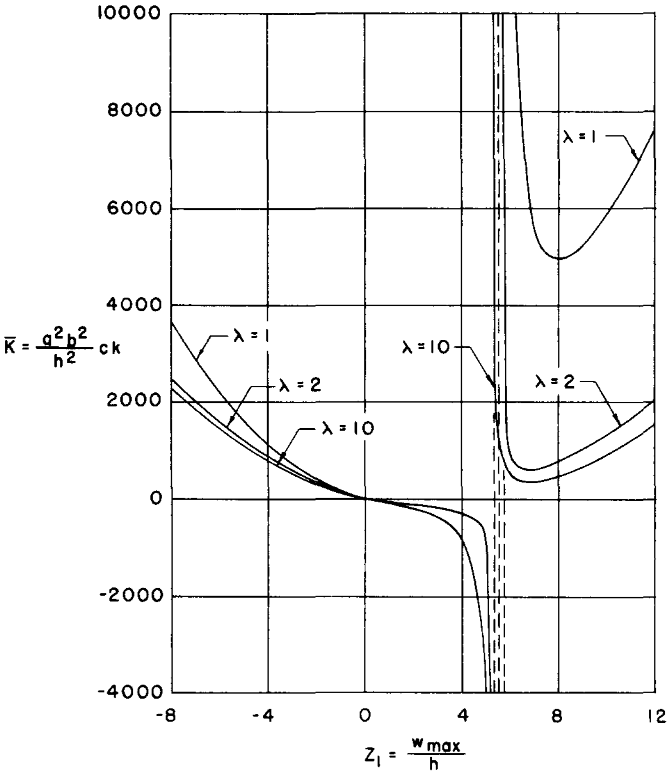


FIG 5. Load–deflection curve for $\mu = 0{\cdot}3$, $K_y = 30$, $\bar{f} = 0$ and $\bar{e}_x = \bar{e}_y = 0$.

The behavior of the shell with restrained edges is studied by plotting the above equation for various values of the curvature $K_y$ and aspect ratio $\lambda$. The resulting graphs are shown in Figs. 4 and 5.

## CONCLUSIONS

The buckling temperature of a thin shallow cylindrical shell panel is found to be a function of the curvature parameter, the dimensions of the shell, and the degree of restraint of the edges.

The graphs obtained show that if the shell is subjected to a temperature difference, which is larger than the critical value, snapbuckling may occur once sufficient perturbations are present to overcome the energy barrier separating the stable equilibrium states.

From the results of the analysis, the following conclusions can be drawn:

(*a*) For the shell, with the edges free to displace in the middle surface, thermal buckling may occur in the practical temperature range even for moderately high curvature parameter; whereas for the shell with restrained edges buckling may occur in the practical temperature range only for small curvature parameters.

(*b*) The value of the maximum deflection $W_{max}$ which corresponds to the critical temperature increases with increased curvature parameter.

(*c*) For the free-edge case the critical temperature difference value increases slightly for higher aspect ratios; whereas for the shell with restrained edges the critical value decreases considerably when the value of the aspect ratio is doubled. This decrease is due to the larger influence of the in-plane edge forces.

(*d*) The use of the first-order solution is quite sufficient for engineering purposes.

*Acknowledgment*—This work was supported in part by the National Aeronautics and Space Administration under Research Grant Ns G-298-62.

The author expresses his gratitude to Dr. H. Zorski of The Institute for Fundamental Engineering Research, Polish Academy of Sciences, for suggesting the problem.

## REFERENCES

[1] M. S. ANDERSON, *NASA tech. Note*, D-1510, pp. 255–266, Dec. (1962).
[2] N. J. HOFF, *J. appl. Mech.* **24**, 405 (1956).
[3] N. J. HOFF, *J. R. Aeronaut. Soc.* **61**, 756 (1957).
[4] D. ABIR and S. V. NARDO, *J. Aeronaut. Sci.* **26**, 803 (1959).
[5] D. J. JOHNS, D. S. HOUGHTON and J. P. H. WEBBER, Coll. Aero. Cranfield, Report 147, p. 29, May (1961).
[6] J. SINGER and N. J. HOFF, *AFOSR*, TR 59–203, p. 82, December (1959).

## APPENDIX

*The values of the coefficients $a_i$, $b_i$, $f_1$ and $f_2$*

The following coefficients are used in equations (17), for the case where $P_x = P_y = 0$.

$$a_1 = \frac{\pi^4}{64}\left(\lambda^2+\frac{1}{\lambda^2}\right)$$

$$a_2 = \pi^2\lambda^2\left[\frac{2{\cdot}327}{(1+\lambda^2)^2}+\frac{0{\cdot}97}{(1+9\lambda^2)^2}+\frac{2{\cdot}91}{(9+\lambda^2)^2}+\frac{0{\cdot}133}{\lambda^4}+0{\cdot}133\right]$$

$$a_3 = -\pi^2\lambda^2K_y\left[\frac{0{\cdot}612}{(1+\lambda^2)^2}+\frac{1}{32}\right]$$

$$a_4 = \pi^4\lambda^2\left[\frac{1}{32\lambda^4}+\frac{1}{4(1+\lambda^2)^2}+\frac{0{\cdot}1874}{(1+9\lambda^2)^2}+\frac{9}{16}\frac{1}{(9+\lambda^2)^2}+\frac{1}{32}\right]$$

$$a_5 = -\lambda^2K_y\left[\frac{8}{3}\frac{1}{(1+\lambda^2)^2}+\frac{1}{6}\right]$$

$$a_6 = \frac{1}{16}\lambda^2K_y\left[-\frac{4{\cdot}64}{(1+\lambda^2)^2}+\frac{0{\cdot}128}{(1+4\lambda^2)^2}+\frac{0{\cdot}71}{(4+\lambda^2)^2}-9{\cdot}6\right]$$

$$a_7 = \frac{\pi^2}{16}\lambda^2\left[\frac{64}{15}\cdot\frac{1}{\lambda^4}+\frac{2{\cdot}86}{(1+\lambda^2)^2}+\frac{0{\cdot}26}{(1+4\lambda^2)^2}+\frac{0{\cdot}26}{(4+\lambda^2)^2}+\frac{64}{15}\right]$$

$$a_8 = \left[\frac{\lambda^2}{4}K_y^2\frac{1}{(1+\lambda^2)^2}+\frac{\pi^4(1+\lambda^2)^2}{48(1-\mu^2)\lambda^2}-\frac{\lambda^2}{16}K\left(\frac{\pi^2}{6}-1\right)\right]$$

$$a_9 = \left[\frac{1}{3}K_y^2\frac{\lambda^2}{\pi^2}+\frac{1}{9}K_y^2\frac{\lambda^2}{\pi^2}\frac{1}{(1+\lambda^2)^2}+\frac{16}{9}\frac{\pi^2}{(1-\mu^2)}\left(\frac{1}{2}+\frac{1}{\lambda^2}+\lambda^2\right)-\frac{2\lambda^2}{3}\bar{K}\left(\frac{1}{3}-\frac{80}{27\pi^2}\right)\right]$$

$$b_1 = \frac{2\pi^2}{15}\left[\frac{1}{\lambda^2}+\lambda^2\right]$$

$$b_2 = \pi^4\lambda^2\left[\frac{1}{4(1+\lambda^2)^2}+\frac{3}{16(1+9\lambda^2)^2}-\frac{1}{128(9+\lambda^2)^2}+\frac{1}{64\lambda^4}+\frac{1}{64}\right]$$

$$b_3 = -\lambda^2 K_y\left[\frac{4\cdot813}{(1+\lambda^2)^2}+\frac{0\cdot1781}{(1+9\lambda^2)^2}-\frac{4\cdot81}{(9+\lambda^2)^2}-\frac{4}{15}\right]$$

$$b_4 = \pi^2\lambda^2\left[\frac{3\cdot05}{(1+\lambda^2)^2}+\frac{0\cdot0167}{(1+4\lambda^2)^2}+\frac{2\cdot87}{(1+9\lambda^2)^2}+\frac{0\cdot0167}{(4+\lambda^2)^2}+\frac{8\cdot66}{(9+\lambda^2)^2}+\frac{4}{15\lambda^4}+\frac{4}{15}\right]$$

$$b_5 = -\pi^2\lambda^2K_y\left[\frac{1}{4(1+\lambda^2)^2}+\frac{1}{64}\right]$$

$$b_6 = -\frac{\pi^2}{32}\lambda^2K_y\left[\frac{3}{2(1+\lambda^2)^2}+2\right]$$

$$b_7 = \frac{\pi^4}{16}\lambda^2\left[\frac{1}{2(1+\lambda^2)^2}+\frac{1}{8(1+4\lambda^2)^2}+\frac{1}{8(4+\lambda^2)^2}+\frac{1}{2\lambda^4}+\frac{1}{2}\right]$$

$$b_8 = \left[\frac{4\pi^2}{27(1-\mu^2)}\frac{(1+\lambda^2)^2}{\lambda^2}+\frac{16}{9}\frac{\lambda^2}{\pi^2}K_y^2\frac{1}{(1+\lambda^2)^2}-\frac{\lambda^2}{3}\bar{K}\left(\frac{1}{3}-\frac{80}{27\pi^2}\right)\right]$$

$$b_9 = \left[\frac{\pi^4}{12(1-\mu^2)}\left\{\frac{3}{4}\left(\frac{1}{\lambda^2}+\lambda^2\right)+\frac{1}{2}\right\}+\frac{1}{32}\lambda^2K_y^2\left(1+\frac{1}{2(1+\lambda^2)^2}\right)-\frac{\lambda^2\bar{K}}{128}\left(\pi^2-\frac{15}{2}\right)\right]$$

$$f_1 = \left[\bar{K}\ \frac{K_y\lambda^2}{\pi^2}\left(\frac{1}{2}-\frac{4}{\pi^2}\right)\right]$$

$$f_2 = \bar{K}\left[\frac{K_y\lambda^2}{16}\left(\frac{1}{6}-\frac{1}{\pi^2}\right)\right].$$

(*Received* 4 *March* 1965)

**Résumé**—Les équations de flexion large d'une enveloppe mince peu profonde y sont modifiées pour inclure les effets thermiques. La température est considérée en tant que fonction arbitraire des coordonnées dans l'espace.

Les équations qui en résultent sont employées pour étudier le comportement du gondolement thermique et l'état de l'après-stabilité d'un panneau d'enveloppe cylindrique à support simple et soumis à une distribution parabolique de la température le long de sa direction axiale. L'on a assumé que la température est constante à travers l'épaisseur de l'enveloppe et le long de sa direction circonférencielle. Des diagrammes de stabilité pour diverses courbures, $K_y$ ainsi que des rapports d'aspect $\lambda$, sont présentés dans deux cas de conditions de rebord. Dans l'un des cas, les rebords du panneau sont libres de se déplacer, et dans le second les rebords sont retenus.

L'on a trouvé que la température critique baisse en dehors de la gamme pratique de température de la matière pour $K_y \geq 200$ dans les conditions de rebords libres, et pour $K_y \geq 50$ dans les conditions de rebords retenus.

**Zusammenfassung**—Die grossen Biegungsgleichungen für eine dünne flache Schale sind abgeändert um Wärmeeinwirkungen einzuschliessen. Die Temperatur ist als eine willkürliche Funktion der Raumkoordinaten erwogen.

Die resultierenden Gleichungen werden für die Untersuchung von Wärmeknickfestigkeit und Nach-Knickfestigkeitsverhalten eines einfach unterstützten zylindrischen Schalen stüches, welches zu einer parabolischen Temperaturverteilung entlang seiner Achsrichtung unterworfen ist, verwendet. Es wird angenommen, dass die Temperatur, quer durch die Dicke der Schale und entlang ihrer Umkreisrichtung konstant ist. Knickfestigkeitstabellen für verschiedene Krümmungen $K_y$ und Streckungsverhältnissen, $\lambda'$ für zwei Fälle von Randbedingungen sind präsentiert. In einem Fall, die Ränder der Schale sind frei für Verschiebung und im zweiten Fall werden die Ränder zurückgehalten.

Es wurde gefunden, dass die kritische Temperatur ausserhalb des praktischen Temperaturbereiches des Materiales fällt für $K_y \geq 200$ im Falle der freien-Randbedingung und für $K_y \geq 50$ im Falle der zurückgehaltenen Randbedingung.

**Абстракт**—Уравнеиия больших изгибов для тонкой поверхностной оболочки изменены для включения термического эффекта. Температура считается произвольной функцией пространственных координат.

Полученные в результате уравнения применяются для изучения термических продолых изгибов и поведения после изгиба обычно поддерживаемой цилиндрической оболочки панели, подвергшейся параболическому распределению температуры вдоль её осевого направления. Принимается, что температура постоянна поперёк толщины оболочки и вдоль её периферического направления. Таблица для продольных прогибов для различных изгибаний $K_y$ и удлинения камеры сгорания $\lambda$ представлены для двух случаев состояния края. В одном случае края панели свободно перемещаются, а во втором случае края ограничиваются.

Найдено, что критическая температура выходит из ряда практической температуры материала для $K_y \geqslant 200$ в условиях свободного края и для $K_y \geqslant 50$ при условии ограниченного края.